Journal of Fluids and Structures (1999) **13,** 967–986
Article No.: jfls. 1999.0245, available online at http://www.idealibrary.com on IDEAL®

THE FLUID AND MECHANICAL COUPLING BETWEEN TWO CIRCULAR CYLINDERS IN TANDEM ARRANGEMENT

A. Laneville and D. Brika

Département de génie mécanique, Université de Sherbrooke, Sherbrooke, Québec, J1K 2R1, Canada

(Received 13 October 1998 and in revised form 7 May 1999)

The effect of the fluid and mechanical coupling between two flexible circular cylinders on their vortex-induced oscillations is examined in a wind tunnel. The cylinders are in a tandem arrangement and a mechanical coupling allows vibrations in phase and out of phase. The separation between the cylinders ranges between 7 and 25 diameters. When the cylinders are coupled only by fluid, the upstream cylinder behaves as an isolated one, while the downstream cylinder response depends on the separation and presents a hysteresis and three discontinuities. The hysteresis and its discontinuities agree with those of the upstream cylinder and the third discontinuity coincides with the end of synchronization of the windward cylinder. The addition of the mechanical coupling complicates the dynamic response which is greatly influenced by the separation and the coupling mode involved. The results are interpreted according to those dealing with the fluid coupling only. The effect of small-scale grid turbulence is also examined.

1. INTRODUCTION

The flow around the downstream cylinder of a tandem arrangement of two cylinders involves a complicated wake produced by the upstream cylinder: the physics of the wake include velocity fluctuations distributed over a wide range of frequencies, thus turbulence driven by flow separation and vortex shedding. This is a variation on the theme of the effects of turbulence on bluff bodies, a theme Professor Yasuharu Nakamura has contributed to. Among the different aspects of bluff body aerodynamics, he was indeed particularly interested in the phenomena of flow separation and the subsequent vortex formation under the influence of external turbulence. During his October 1989 visit to Sherbrooke, the discussions focused on the observation of the 2S-2P modes of vortex shedding and had he returned, the discussions would certainly have turned to the mechanism involved in the flow around the downstream cylinder. According to Professor Nakamura (Nakamura 1993; Nakamura & Ohya 1986; Nakamura & Hirata 1989), there are "two main modules in bluff body flow": flow separation and reattachment on the one hand and formation of the wake of vortices on the other. Therefore, external "turbulence can exert a strong influence on the near wake flow if its scale is comparable to either the shear layer thickness or the spacing between the two shear layers (more simply the cylinder size)". Small-scale turbulence has a direct local interaction on the shear layer/edge, while large-scale turbulence modifies the spanwise correlation of the vortex formation (Nakamura & Ohya 1986).

In this paper, data mainly taken from the authors' own wind tunnel measurements of vortex-induced vibrations of cylinders in tandem will be discussed in terms of the vortex formation: they are part of a long-term research investigation, based on pure experimental

0889–9746/99/100967 + 20 $30.00

grounds, the objective of which was, and still is, to gain a better knowledge of the different phenomena to which transmission lines are submitted in smooth and turbulent flows. The phenomenon of vortex-induced vibrations was of prime concern because of its frequent occurrence and the fatigue damage it produced. This phenomenon experienced by cables is a well-known aeroelastic instability that occurs when the frequency of the shed vortices, f_{vs}, matches one of the resonance frequencies, f_n, of the cables system. This matching is established for a given cable with diameter D, at the critical fluid velocity, V_{cr}, defined by an equivalent Strouhal number, St (0·19 for a circular cylinder), $V_{cr} = f_n D/\mathrm{St}$, but experimental observations in the case of a single flexible cable with a circular shape indicate that the synchronization of the vortex shedding frequency with f_n occurs over a domain of fluid velocities $0{\cdot}8 < V/V_{cr} < 1{\cdot}2$.

The different cases studied in this research program were: (a) a flexible cylinder vibrating orthogonally in cross-flow, (b) a flexible cylinder vibrating non-orthogonally in cross-flow, (c) a flexible cylinder downstream of a stationary one, (d) two flexible cylinders both free to vibrate, (e) two flexible cylinders coupled mechanically, and (f) the effect of external turbulence. In this paper, dealing with a tandem configuration of cylinders, results obtained in parts (d)–(f) will be discussed using the observations made in the case of the isolated cylinder in cross-flow and downstream of a stationary one. The questions raised are as follows:

(i) What is the response of a free flexible cylinder (the downstream one) when submitted to a "stationary" wake convecting vortices at a frequency that varies with the oncoming flow velocity?

(ii) What is the response of the same cylinder if the wake undulates with the motion of the upstream flexible cylinder and convects vortices that are at a single frequency, its resonance frequency? In this configuration of aerodynamically coupled cylinders, is there a "natural" phase difference between the response of the upstream and downstream cylinders?

(iii) When the flexible cylinders are mechanically coupled, is the overall response influenced by an imposed phase difference that differs from the "natural" one observed when the cylinders are only coupled aerodynamically?

(iv) What is the effect of small scale turbulence structures on the response of the mechanically coupled tandem cylinders as well as on the modes of vortex shedding?

2. EXPERIMENTAL SET-UP

In this research program, the experimental set-up, especially the dimension and the elastic properties of flexible cylinders had to be maintained or modified at the minimum. The extraneous effects such as blockage, and end-effects had also to be kept to a minimum.

The experimental set-up using an isolated flexible cylinder is described in more detail in Brika & Laneville (1993). It consists of a long tube suspended horizontally in a wind tunnel by thin steel flexible blades at the nodes of its first free–free vibration mode. The length of the model ($l = 3{\cdot}313$ m) is chosen such that the nodes are located exactly at the tunnel walls. The part of the model internal to the wind tunnel vibrates in a quasi-sinusoidal mode shape. The tube has an external diameter $D = 33{\cdot}4$ mm, a natural frequency $f_n = 17{\cdot}58$ Hz of its first free–free vibration mode and a mass per unit length $m_l = 0{\cdot}864$ kg/m. The cylinder displacement is measured with a B & K 4393 accelerometer and the velocity fluctuations downstream the cylinder are monitored with a TSI hot wire anemometer. The spectral analysis of both signals are performed on B & K 2032 frequency analyzer. A shaker (B & K 4809) is also used to pump up the cylinder to a high amplitude for some tests. The advantages of the present experimental set-up are as follows: (i) low damping ratio,

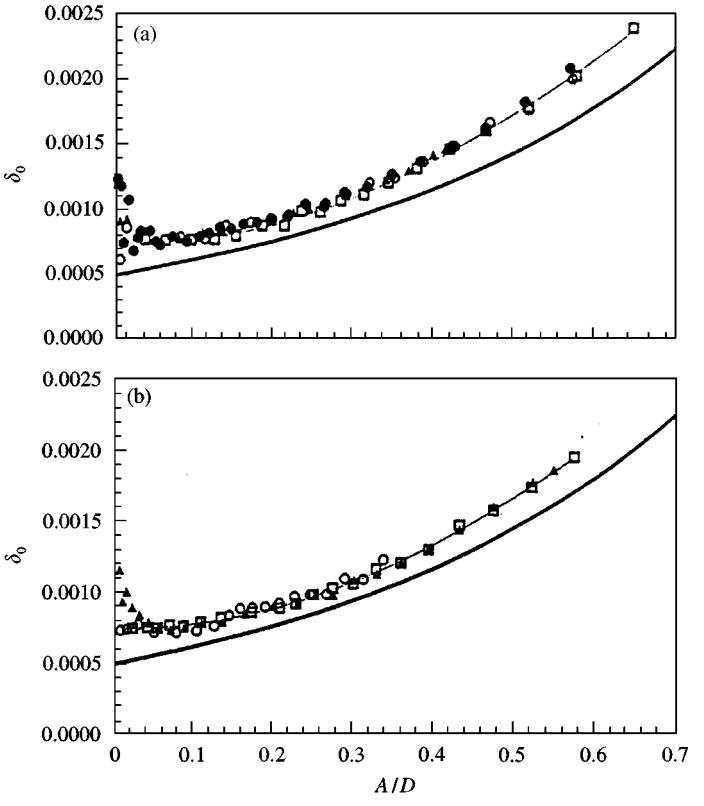

Figure 1. Logarithmic decrement of the mechanically coupled flexible cylinders in still air as a function of the amplitude A/D: (a) in-phase motion; (b) out-of-phase motion.

$\zeta = 0{\cdot}8 \times 10^{-4}$, (ii) low blockage ratio, $D/H = 1{\cdot}8\%$ (H is the height of the wind tunnel test section), (iii) high aspect ratio $l_w/D = 52{\cdot}7$ (l_w is the length of the model exposed to wind), (iv) spanwise simulation of the vibrating transmission lines and (v) reduction of the end-effects.

For parts of the investigation dealing with cylinders in tandem, this basic experimental set-up has been expanded to include a second identical flexible circular cylinder, also suspended in the wind tunnel by thin steel flexible blades at the nodes of its first free–free vibration mode. Finally, a coupling mechanism consisting of wire and pulleys has been added to this experimental set-up to force the cylinders to vibrate in phase or out of phase. Before coupling, the natural frequency of each uncoupled cylinder was tuned to $f_n = 17{\cdot}58$ Hz. Once the cylinders were coupled, f_n was reduced to 17·42 Hz. Figure 1 shows the logarithmic decrement in still air, δ_0, as a function of the amplitude of vibration when the coupled cylinders vibrate (a) in phase and (b) out of phase at a spacing ratio $L/D = 13$. The solid bold line illustrates the logarithmic decrement for an isolated cylinder. The curve δ_0 of the coupled cylinders is only shifted to higher values due to additional damping introduced by the bearings and the wires sliding on the pulleys. The system logarithmic decrement is $\delta_m = 7 \times 10^{-4}$ giving a damping $\zeta_m = 1{\cdot}10 \times 10^{-4}$, compared to $\zeta_m = 0{\cdot}8 \times 10^{-4}$ for uncoupled cylinders. The coupling mechanism increases the system damping ratio by 40%. The figure indicates also that the coupling mode does not affect the logarithmic decrement in still air. For the tandem arrangement the separation between the centre of the cylinders was varied between 10 and 25 diameters. In addition to the smooth flow condition, three

turbulence intensities (Tu = 5, 10 and 15%) were superimposed by means of square mesh grids.

3. PREVIOUS OBSERVATIONS

3.1. Single Cylinder Vibrating Orthogonally in Cross-flow

For comparison purposes, Figure 2 summarizes the results obtained with an isolated cylinder by Brika & Laneville (1993) and presents the nondimensional amplitude A/D as a function of the reduced velocity $V_r = V/fD = 2\pi U$, where A is the single amplitude of vibration at the model mid-span, V the mean flow velocity, and f the cylinder vibrating frequency

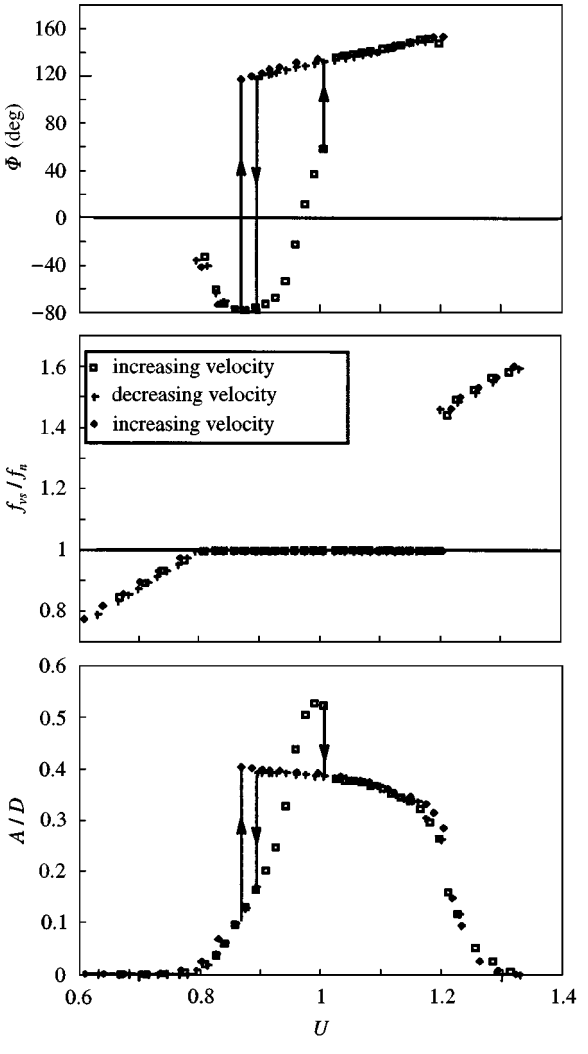

Figure 2. Observation of the hysteretic response of the isolated cylinder in the synchronization region and the coincident lock-in of the vortex shedding frequency and jump in the phase difference between the vortex shedding and cylinder response.

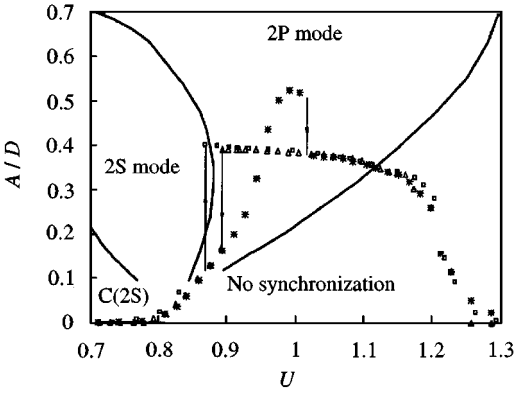

Figure 3. The different modes of vortex shedding and the response of an isolated flexible cylinder: ∗, increasing velocity; Δ, □, decreasing velocity; —, Williamson & Roshko (1988).

($f \approx f_n = 17{\cdot}58$ Hz). The hysteresis phenomenon in the response of the model is characterized with two branches and two discontinuities. Within the range $0{\cdot}8 < U < 1{\cdot}2$, the vortex shedding frequency, f_{vs}, is not given by the Strouhal number and is locked to the cylinder vibrating frequency f ($f_{vs} = f \approx f_n$). In this synchronization region, both, the amplitude $A/D(U)$ and the phase angle $\Phi(U)$ show an hysteresis behaviour characterized by two branches, each delimited by a discontinuity. The value of the steady state $A/D(U)$ and $\Phi(U)$, or the choice between the first or the second branch of the hysteresis loop depends on the cylinder motion history as well as on the initial conditions (Brika & Laneville 1993). The first branch, obtained with a progressive increase of the flow velocity (small steps), extends from the synchronization onset velocity $U \approx 0{\cdot}78$ to the upper critical velocity $U = 1{\cdot}02$, when a jump to the second branch occurs. The second branch, which extends from the end of synchronization $U = 1{\cdot}2$ to the lower critical velocity $U \approx 0{\cdot}88$, is generally obtained with a progressive decrease of flow velocity. Similar results have been obtained by Feng (1968) for the smallest damping ratios $\zeta = 0{\cdot}00135$ and $0{\cdot}00181$ and are discussed in detail in Brika & Laneville (1993). The hysteresis loop of the present study covers a velocity range twice as large as that observed by Feng (1968). It is interesting to note that both, amplitude and phase angle Φ, vary rapidly with U on the first branch, while on the second branch, they vary slightly with U; the amplitude of vibrations A/D correlates well with the phase angle between the excitation and the cylinder displacement.

Flow visualization (Brika & Laneville 1993) has shown that each branch of the hysteresis loop is associated with a particular vortex pattern in the wake of the cylinder and each discontinuity is attributed to a sudden change from one mode of vortices to another, supporting the hypothesis previously advanced by Williamson & Roshko (1988) and the observations of Zdravkovich (1982). The first branch, generally obtained with a progressive increase of the flow velocity and ranging between the synchronization onset velocity and the resonance velocity, is associated with the so-called 2S mode (Williamson & Roshko 1988) where a single vortex is shed from each side of the cylinder at every cycle of vibration like the natural Karman vortices (see Figure 3). The second branch, ranging between the end of synchronization and $V_r = 5{\cdot}5$ and generally obtained with a progressive decrease of the reduced velocity, is associated with another vortex pattern referred to as the 2P mode where a pair of vortices of opposite signs are shed from each side of the cylinder at every cycle of vibration.

3.2. Effects of an Upstream Stationary Cylinder

The presence of an upstream cylinder, either stationary or free to vibrate will now be discussed. The experimental results were obtained by Brika & Laneville (1999). Figure 4 shows the effect of the spacing ratio L/D on the dynamic response of the downstream cylinder A/D as a function of the reduced velocity V_r in the case of the progressive regime. In comparison with the results of an isolated cylinder, the dynamic response is no more hysteretic and the jumps in the oscillation amplitude have completely disappeared. The results of Figure 4 also indicate that (a) due to the shielding effect, the synchronization onset occurs at a higher reduced velocity than that of an isolated one and (b) the synchronization region is much larger and decreases with increasing value of L/D. For $L/D = 10$, say, the synchronization region is twice as large as that of an isolated cylinder. The expansion of the synchronization region occurs essentially at higher reduced velocities. The maximum amplitude as well as the velocity for which this maximum occurs (resonance velocity, V_R) also decrease with increasing L/D. Up to the largest spacing ratio tested ($L/D = 25$), the leeward cylinder response remains different from the one of a single cylinder, and the upstream cylinder can be said to still influence the response of the downstream one. The maximum amplitude of oscillations is roughly of the same order as that of an isolated cylinder but with higher values at small spacing ratios and lower values at large separations. The results of Figure 4 also indicate the presence of a first peak with $A/D < 0{\cdot}06$ around the reduced velocity $V_r = 5$. In the neighbourhood of this velocity, the vortices shed from the upstream cylinder have a frequency approximately equal to the natural frequency of the downstream cylinder and as they impinge on the leeward cylinder they trigger its oscillation. As the vortices of the stationary upstream cylinder cannot lock-in to the vibrating frequency of the downstream model, this oscillation amplitude vanishes with increasing value of the reduced velocity.

The results of Figure 4 show that for a given mean flow velocity in the range defined by the synchronization onset velocity and $V_r = 6{\cdot}7$, the amplitude of oscillations remains roughly the same for all the spacing ratios examined. For velocities larger than V_R, the effect of L/D can be seen to reduce the amplitude of oscillations at a given velocity. For each spacing ratio, the amplitude A/D increases more rapidly with V_r before resonance, and

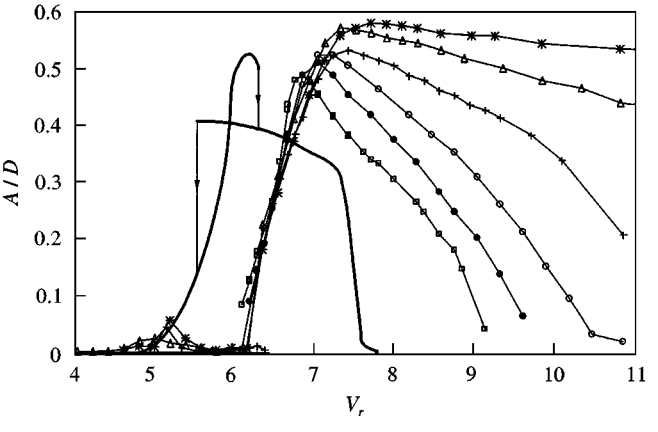

Figure 4. The effect of an upstream stationary cylinder on the response of a flexible cylinder at different downstream locations L/D: ∗: 7, Δ: 9, + : 10, ○; 13, ●: 16, □: 25, —: isolated cylinder.

decreases in a more progressive manner past the resonant velocity. A point of inflection, more apparent for $L/D = 25$ ($V_r = 7{\cdot}25$, $A/D = 0{\cdot}41$), can be observed just past the resonance. Because of these differences of behaviour prior to and after the resonance velocity and taking into account the results of the isolated cylinder, it can be deduced that two different vortex patterns can be present in the wake of the downstream cylinder, even if no hysteresis phenomenon is observed in its dynamic response. The velocity where a progressive jump from one vortex pattern to another occurs is expected to be around the resonance velocity. This hypothesis is verified with flow visualization (Brika & Laneville 1999).

4. AERODYNAMIC COUPLING

Figure 5 presents the dynamic response of two cylinders in tandem with a spacing of $L/D = 10$. Both cylinders are self-excited by the flow and coupled aerodynamically only. A_1 and A_2 are, respectively, the amplitude of vibration of the upstream and the downstream cylinder, Φ the phase angle between the vortex shedding and the displacement of the downstream cylinder, and Θ the phase angle between the displacements of the cylinders.

As shown in Figure 5, the response of the upstream cylinder is similar to that of an isolated cylinder, with its hysteresis and two discontinuities. The response of the downstream cylinder is, however, different and presents a hysteresis in A_2, Φ and Θ: the first two discontinuities of this hysteresis concur with those of the upstream cylinder. A_2 and Φ present also a third discontinuity coinciding with the end of synchronization of the upstream cylinder. The phase angle Φ_2 of the lower branch varies now significantly with the reduced velocity contrary to the case of an isolated cylinder where it varies slightly with V_r. The phase Φ_2 flattens and becomes similar to that of an isolated cylinder beyond the end of synchronization of the upstream cylinder. It is worthwhile mentioning that the downstream cylinder presents a growing beating phenomenon prior to the discontinuity at $V_r = 6{\cdot}3$. This beating vanishes beyond the discontinuity. The amplitude A_2 shows a maximum amplitude of oscillation between the second and third discontinuities. The velocity at which this maximum occurs increases with increasing separation between the cylinders, contrary to the case when the upstream cylinder is stationary (see Figure 4). The resonance velocity of the downstream cylinder is lower when the upstream cylinder is vibrating than when it is stationary.

Contrary to the case of a tandem arrangement with a stationary upstream cylinder, for which the synchronization of the downstream cylinder begins at $V_r = 6{\cdot}0$, both cylinders in tandem coupled aerodynamically initiate their oscillation at the same reduced velocity $V_r = 5$. In one case, a "stationary" wake carries vortices, the frequency of which varies with the oncoming flow velocity, in the other case, the wake undulates with the motion of the upstream cylinder and carries vortices of the 2S or 2P type (according to the value of V_r), synchronized at a single frequency that matches the resonance frequency of the downstream cylinder. The latter is of course a very special case, but it is also the worst case. Because of the shielding effect (or the lower flow velocity in the wake) produced by the upstream cylinder, the vortices in the wake of the downstream cylinder should have been shed at a lower frequency than that of the impinging vortices shed by the upstream cylinder: the downstream cylinder then enters in vibration at $V_r = 5$, not 6·0, because the synchronized vortices of the upstream cylinder initiate its vibration at the same velocity as that of the upstream cylinder.

In the case of a tandem arrangement with a stationary upstream cylinder, a first peak around $V_r = 5$ was also observed in A_2, but since the frequency of the vortices shed by the upstream cylinder differs from the natural frequency of the cylinders as the flow velocity is progressively increased, this peak quickly vanished. In the case of a tandem arrangement

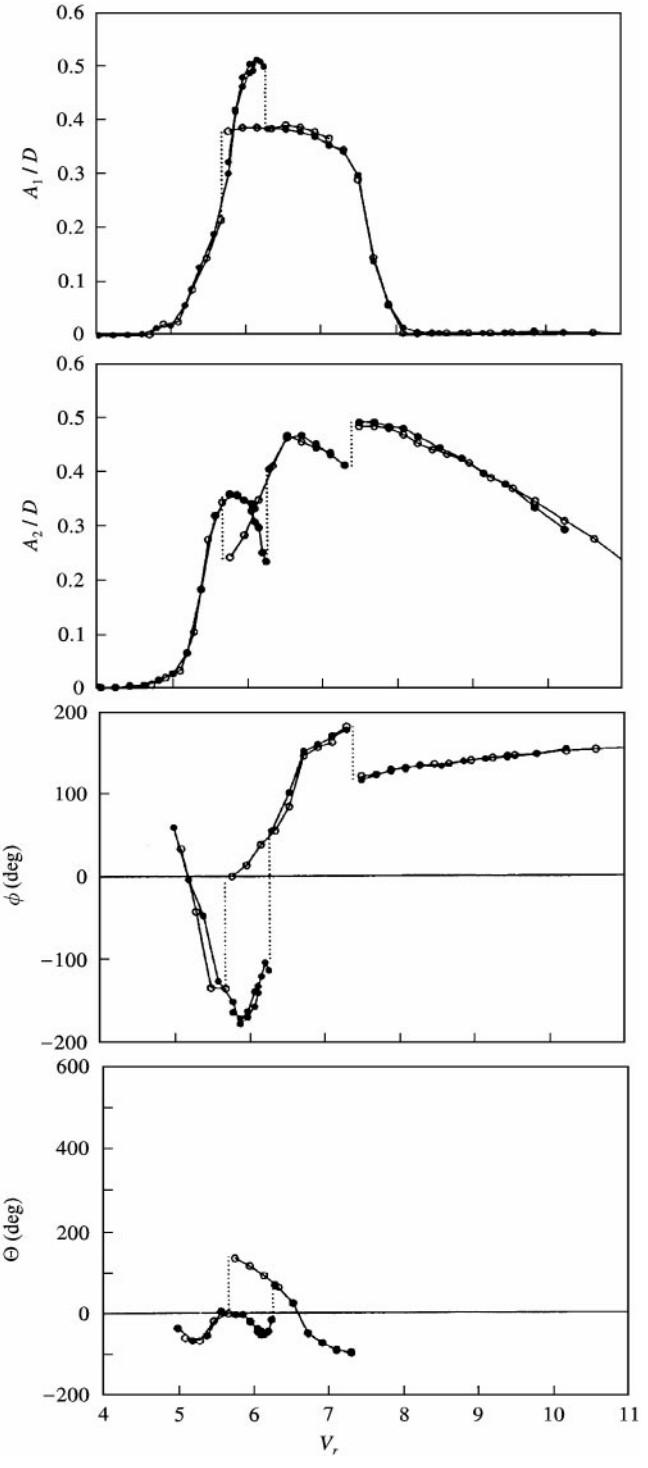

Figure 5. Aerodynamic coupling between two identical flexible cylinders ($L/D = 10$): A_1/D_1, A_2/D_2 are respectively the response of upstream and downstream cylinders, Φ, the phase difference between the vortex shedding and the response of the downstream cylinder, and Θ the phase difference between the response of the two cylinders.

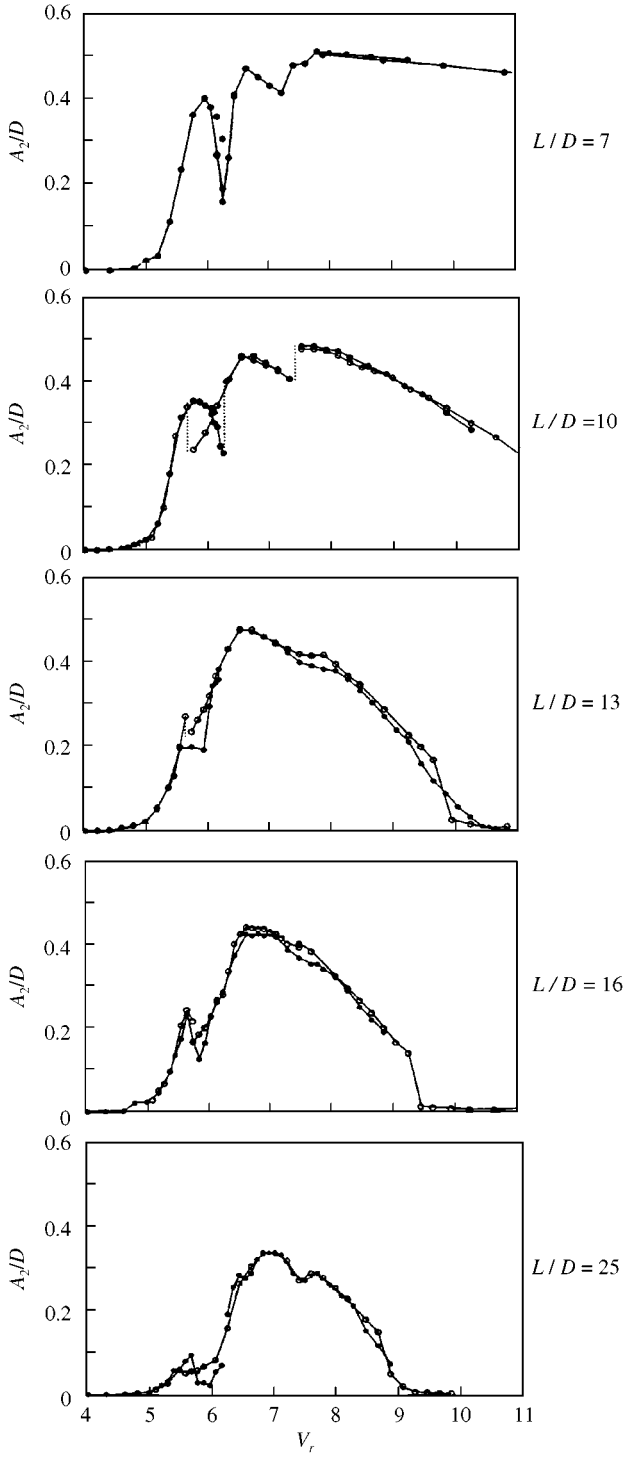

Figure 6. Aerodynamic coupling: the response of the downstream cylinder at different in-line locations: from top, $L/D = 7$, 10, 13, 16, 25.

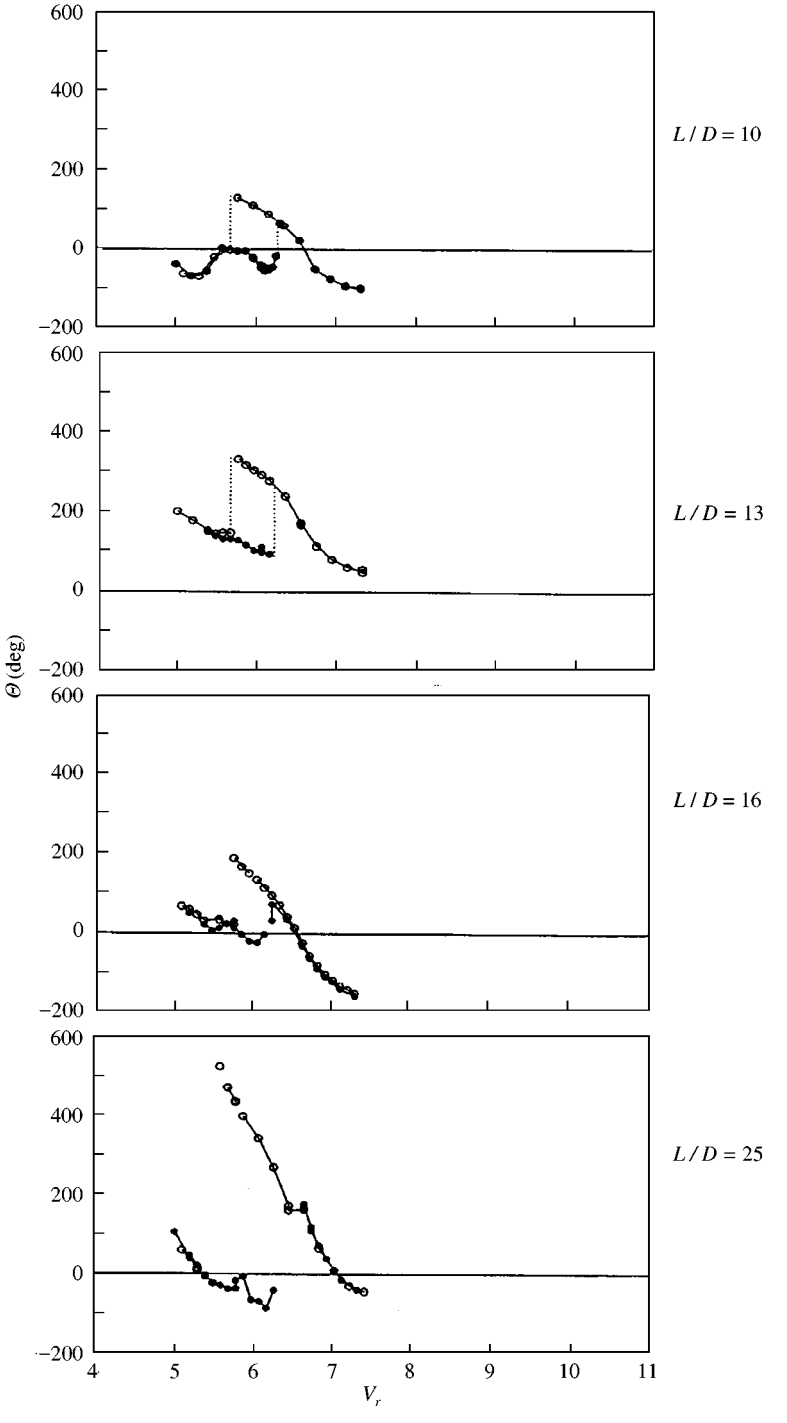

Figure 7. Aerodynamic coupling: the phase difference between the response of the two flexible cylinder separated by different L/D spacing ratios from top, $L/D = 10, 13, 16, 25$.

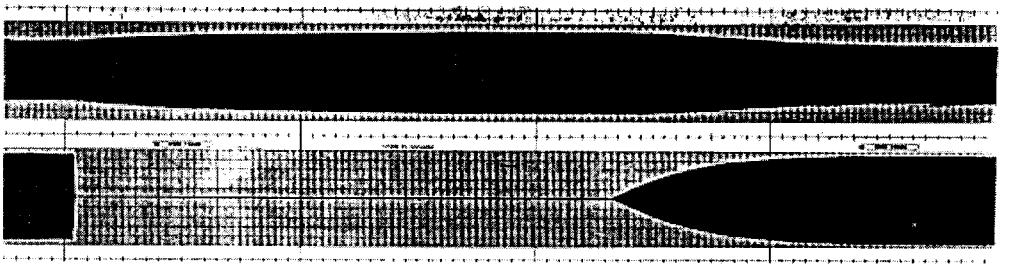

Figure 8. Effect of the downstream cylinder on the response of the upstream cylinder in the case of $L/D = 7$.

with two free flexible cylinders, the peak initiated around $V_r = 5$ does not vanish but continues growing, since the vortices of the upstream cylinder remain synchronized with its natural frequency over a range of flow velocities.

Figures 6 and 7 illustrate the effect of the spacing ratio L/D, respectively, on A_2 and Θ. All these characteristics present a hysteresis with two discontinuities and a third one coinciding with the end of synchronization of the upstream cylinder for all values of L/D examined. The first two discontinuities occur approximately at the same values of V_r as those of the upstream cylinder, and hence as those of an isolated cylinder. Figure 6 shows that the amplitude of vibration A_2 decreases with increasing value of L/D, and this is so for all velocities of the synchronization region. For each separation, the amplitude curve is enveloped by the curve of the previous separation. Figure 6 also shows that the end of synchronization as well as its range decrease with L/D.

The responses of the free cylinders can be seen to have a "preferred" or "natural" phase angle Θ for the different flow velocities and spacing ratios. These data, scarcely available, could be useful in a model as well as for developing means to damp the vibrations.

The response of the downstream cylinder in a tandem arrangement of free flexible cylinders is then significantly affected by the presence of the upstream one which behaves as an isolated one.

In a tandem arrangement made up of an upstream free flexible cylinder and a stationary downstream cylinder, the response of the upstream cylinder can differ from that of an isolated free cylinder especially at relatively small separations (such as $L/D = 7$). This is shown in Figure 8. When both cylinders are vibrating with their steady-state amplitudes, the windward cylinder has an amplitude $A_1/D = 0{\cdot}38$. If the downward cylinder is brought to rest, its amplitude increases to a new value $A_1/D = 0{\cdot}47$. When the downstream cylinder is released, A_1 decreases to its previous steady-state amplitude as A_2 grows from rest. The flow in the near-wake can be influenced by downstream conditions as it may be expected in any subsonic flow.

5. MECHANICAL COUPLING

When mechanical coupling between the cylinders is added to the fluid coupling, the phenomena become more complex. At this stage of this experimental investigation, it is not obvious that the response of two tandem flexible cylinders submitted simultaneously to two different types of coupling will not be chaotic. The results of the previous section have shown that the "natural" phase angle between the displacements of the cylinders is strongly dependent on the flow velocity. When forcing the vibration to be in phase or out of phase (or in a phase that differs from its "natural" one), this means that only part of the total fluid

energy "naturally" imparted to the cylinders is used to excite them, the other part being absorbed by the system. It is foreseeable also that, in this case, the most favourable vibrations are those for which $\Theta = 0$ or 180°.

5.1. Tandem Arrangement with $L/D = 25$, $\Theta_M = 180^\circ$, Progressive Increments of Flow Velocity

Figure 9 shows the response of two coupled cylinders vibrating out of phase ($\Theta_M = 180^\circ$) and separated by a distance of 25 diameters. The response has several peaks and presents a hysteresis with two discontinuities at $V_r = 5{\cdot}7$ and $6{\cdot}3$. These discontinuities match those of an isolated cylinder undergoing an instantaneous change of the vortex pattern from mode 2P to mode 2S at $V_r = 5{\cdot}7$ and *vice versa* at $6{\cdot}3$. The end of synchronization coincides with that of an isolated cylinder, while the synchronization onset is at $V_r = 5$. As the "natural" phase angle between the displacements of two free vibrating cylinders is almost zero around $V_r = 5$ [Figure 7(d)] and as the power imparted by the flow is less important at the beginning of synchronization, the amplitude of vibration around $V_r = 5$ is negligible. The tandem, mechanically coupled cylinders begin to oscillate with appreciable amplitudes around $V_r = 5{\cdot}5$, when the "natural" Θ departs from zero and the power input becomes more important. The amplitude follows the upper branch of the hysteresis and the mode of vortex shedding should resemble the 2S type as the flow velocity is progressively increased. With increasing value of V_r, the "natural" value of Θ [Figure 7(d)] decreases until it jumps ($V_r = 6{\cdot}3$) by almost 360°, from a negative to a positive value larger than the one imposed by the mechanical set-up. Simultaneously, the mode of vortex shedding jumps from the 2S to the 2P types. In the case of the mechanically coupled cylinders, a discontinuity from $A/D = 0{\cdot}34$ to $0{\cdot}265$ is also observed for $V_r = 6{\cdot}3$ (Figure 9). Past this velocity, the amplitude of the tandem system follows the second branch of the hysteresis. The "natural" Θ matches 180° around $V_r = 6{\cdot}7$ with $A_1/D = 0{\cdot}4$ and $A_2/D = 0{\cdot}35$. The maximum amplitude of the mechanically coupled cylinders, $A/D = 0{\cdot}43$, is also reached at $V_r = 6{\cdot}7$. Beyond this last velocity, the "natural" A_1/D, A_2/D and Θ decrease and so does A/D of the mechanically coupled cylinders up to $V_r = 7$. At $V_r = 7$, $\Theta \approx 0^\circ$ and the upstream cylinder, if free, would

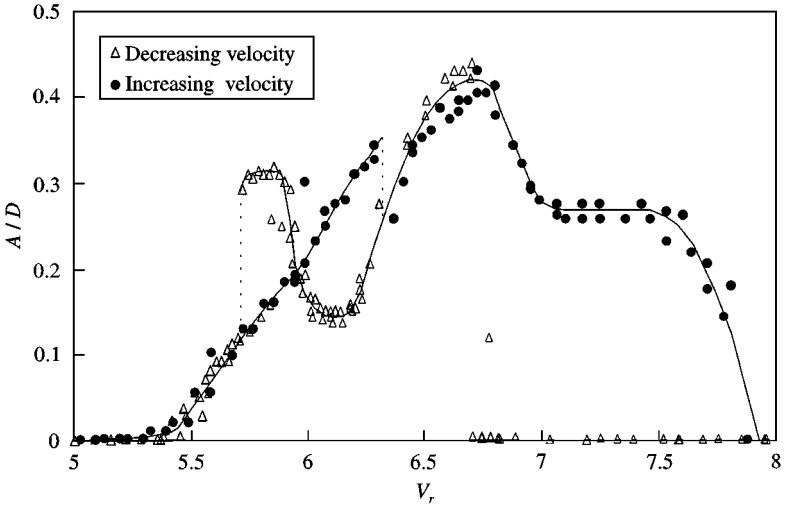

Figure 9. Out-of-phase mechanical coupling ($\Theta_M = 180^\circ$): the response of the tandem system ($L/D = 25$) to a progressive variation of the flow velocity.

tend to come to rest while the downstream one would keep on vibrating (wake galloping). The downstream cylinder drives the tandem system and A/D flattens. At the end of this plateau ($V_r = 7{\cdot}4$), the amplitude A/D decreases rapidly with V_r and the synchronization ends at $V_r = 7{\cdot}8$. For the uncoupled cylinders, synchronization ends at $V_r = 9$.

5.2. Tandem Arrangement with $L/D = 25$, $\Theta_M = 180°$, Progressive Decrements of Flow Velocity

As the flow velocity is reduced in the post-synchronized range and the mode of vortex shedding departs from a nonsynchronized towards one resembling a 2P type (Figure 3), the tandem system of mechanically coupled cylinders, according to the results of Section 5.1, should be triggered in vibration around $V_r = 7{\cdot}8$. The data of Figure 9 for progressive decrements of the flow velocity indicate an onset at a lower value ($V_r = 6{\cdot}7$), that is when the "natural" Θ matches 180°. This observation is puzzling. Unless the energy imparted by the 2P mode is insufficient in the range $6{\cdot}7 < V_r < 7{\cdot}8$ to annihilate the system damping and to bring the tandem system into motion, the steady-state amplitude should be similar to the one observed in the case of progressive increments of the flow velocity. Indeed, the results of additional tests, presented in Figure 10, show that the amplitudes are similar in this range of velocities but require a longer time to reach steady state. as the flow velocity is progressively lowered, the mode of vortex shedding resembling the 2P type should persist down to the "natural" flow velocity for the 2P-2S jump. The lower branch of the hysteresis in the case of the mechanically coupled tandem ends around $V_r = 5{\cdot}7$, in agreement. The minimum of this lower branch occurs at $V_r = 6{\cdot}1$: this flow velocity corresponds to the one for which the free downstream cylinder is almost at rest. In these conditions the upstream cylinder drives the tandem system.

5.3. Tandem Arrangement with $L/D = 25$, $\Theta_M = 180°$, Impulsive Onsets

Figure 10 shows the steady-state amplitude of the cylinders when they are released from rest or from an initial amplitude $A_i/D = 0{\cdot}25$ or $0{\cdot}6$ pumped up with a shaker. Most of the results

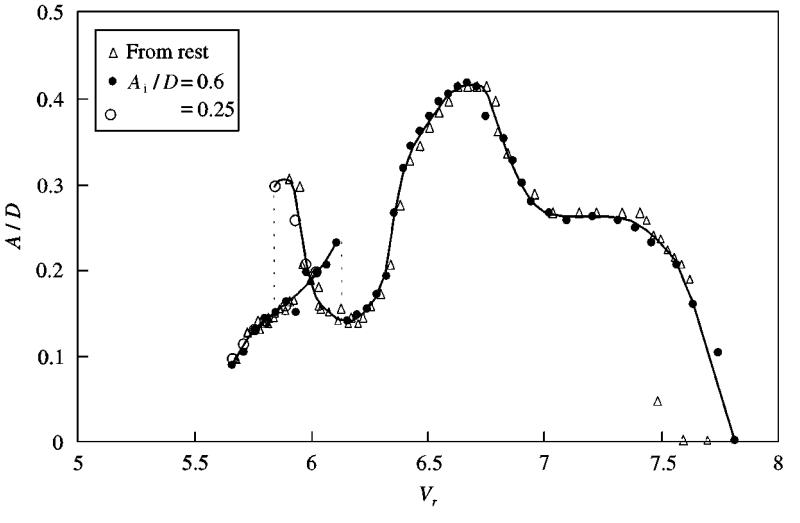

Figure 10. Out-of-phase mechanical coupling ($\Theta_M = 180°$): the response of the tandem system ($L/D = 25$) to impulse onset.

of Figure 9 are reproduced, except the results around the discontinuities, indicating that their positions are the most critical. The steady-state amplitudes obtained from rest or from a high amplitude are always the same, except in the hysteresis region: one branch is obtained from rest or $A_i/D = 0{\cdot}25$ and the other from $A_i/D = 0{\cdot}6$.

5.4. Tandem Arrangement with $L/D = 25$, $\Theta_M = 0^\circ$, Progressive Variations of Flow Velocity

When the tandem cylinders are forced to vibrate in phase, their amplitude of oscillation shown in Figure 11 completely differs from that in Figure 9 ($\Theta_M = 180^\circ$). For this particular case, the hysteresis phenomenon is absent and the dynamic response is identical either with increasing or decreasing velocity. The amplitude curve shows three peaks respectively at $V_r = 5{\cdot}8$, $6{\cdot}4$ and $7{\cdot}2$. At $V_r = 5{\cdot}8$ and $7{\cdot}2$, Θ is approximately zero and at this last value $A_1 = A_2 = A = 0{\cdot}35D$ confirming the fact that all the three characteristics A_1, A_2 and Θ of the aerodynamic coupling are combined when considering the mechanical coupling. At $V_r = 6{\cdot}4$, $\Theta \approx 320^\circ$, A_1 and A_2 of the aerodynamically coupled cylinders are, respectively, $0{\cdot}4$ and $0{\cdot}26$ and the amplitude of the mechanically coupled cylinders is $0{\cdot}32$ which is roughly equal to the average of A_1 and A_2.

The velocity $V_r = 6{\cdot}65$ for which a minimum amplitude occurs ($A/D = 0{\cdot}2$) corresponds to the one where $\Theta_a = 180^\circ$ for the free vibrating cylinders. This situation is the most disadvantageous one for the in-phase mode of mechanical coupling. For the free vibrating cylinders and around this velocity, the downstream cylinder has a maximum amplitude $A_2/D = 0{\cdot}33$ while the upstream one has an amplitude $A_1/D = 0{\cdot}38$. Beyond $V_r = 7$, Θ, as shown in Figure 7, departs from zero, the upstream cylinder is at its upper limit of the synchronization region and its amplitude comes sharply to rest. When mechanically coupled with the downstream cylinder, it restrains the motion of the latter and brings the tandem system to rest at $V_r = 7{\cdot}2$. When the cylinders are coupled only by fluid, the downstream cylinder comes to rest around $V_r = 9$ as shown in Figure 6. Beyond the end of synchronization of the upstream cylinder, the downstream cylinder behaves as a free

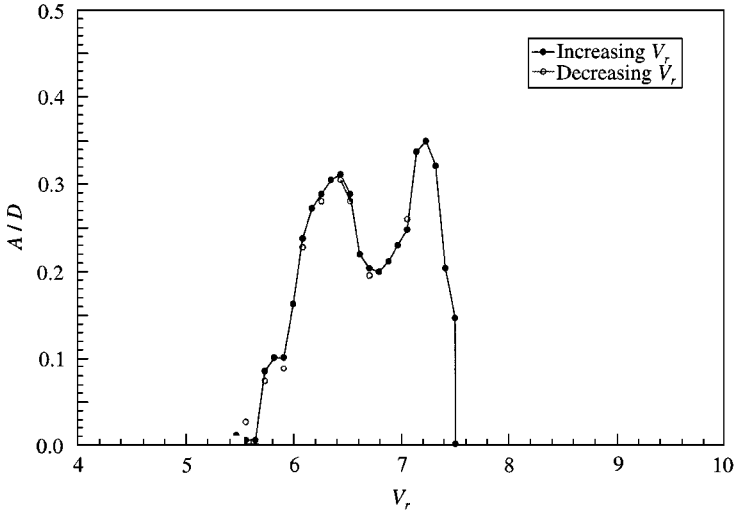

Figure 11. In-phase mechanical coupling ($\Theta_M = 0^\circ$): the response of the tandem (L/D) = 25) to a progressive variation of the flow velocity.

cylinder vibrating in the wake of a fixed cylinder (see Figure 4). Since the power imparted by wind to a cylinder vibrating in the wake of a stationary cylinder is maximum around the resonance at $V_r = 6{\cdot}8$ (Brika & Laneville 1996, 1997) and then significantly reduced for $V_r \geq 7{\cdot}2$, and, since the power input is negligible for the upstream cylinder at rest, in this range, it is then foreseeable that the mechanically coupled cylinders come to rest beyond $V_r = 7{\cdot}2$.

5.5. Tandem Arrangement with $L/D = 25$, $\Theta_M = 0^\circ$, Impulsive Onsets

When the mechanically coupled cylinders are released from rest or from a high amplitude initially pumped up with a shaker, they always stabilize on the curve shown in Figure 11.

5.6. Effect of the Spacing Ratio L/D

Figures 12 and 13 show the effect of the separation L/D on the dynamic response of the coupled cylinders vibrating respectively in phase and out of phase. No common tendency can be deduced on the effect of L/D from this figure. The results can be explained according to those of the aerodynamically coupled cylinders given in Figures 6 and 7. The amplitude A/D of the coupled cylinders results from a combination of A_1, A_2 and Θ of the aerodynamically coupled cylinders. In all cases, however, there is a discontinuity around $V_r = 6{\cdot}3$ concurring with the upper discontinuity of an isolated cylinder which shows an instantaneous change of the vortex pattern from the 2S to the 2P mode. For the coupled cylinders vibrating in phase, we can observe a discontinuity ($L/D = 10$ and 16) or a minimum amplitude ($L/D = 13$ and 25) around $V_r = 6{\cdot}7$. The minimum occurs when $\Theta \approx 180^\circ$ while the discontinuity is present when Θ is roughly 90°. For $L/D = 13$ and $V_r = 8$, there is curiously a peak of the same order of amplitude of that for a cylinder vibrating freely in the wake of another cylinder. At this velocity, the upstream cylinder is outside its synchronization region. For each separation, the end of synchronization of the mechanically and aerodynamically coupled cylinders is lower than that for cylinders coupled only by fluid. This may be attributed to the increase of the damping ratio of the system but also to the fact that beyond the end of synchronization of the upstream cylinder ($V_r = 7{\cdot}2$), the driving cylinder is the downstream one only, and the power input available is then divided between the two cylinders.

For the coupled cylinders vibrating out-of-phase (see Figure 13), the effect is somewhat reversed with respect to the spacing ratio and also to the coupling mode; i.e. the response at $L/D = 10$ and $\Theta_M = 0^\circ$ is similar to that of the case ($L/D = 13$, $\Theta_M = 180^\circ$) and *vice versa*. The same remark applies approximately for $L/D = 16$ and 25.

5.7. Effect of Small-Scale Turbulence

The two variables generally used to describe the turbulence are its intensity, i.e. the r.m.s. value of the velocity fluctuations compared to the time mean velocity value, and its macro-scale related to the characteristic dimension of the structure.

Laneville and Parkinson (1971) have observed that the intensity of turbulence plays a more important role in the vibrations of bluff bodies than the turbulence scale. In the particular case of a circular cylinder, Surry (1969) had also observed an important increase of the r.m.s. value of the lift force and a decrease of the drag with increasing value of the turbulence intensity. The mechanism lying behind this behaviour as suggested in Laneville, Gartshore and Parkinson (1975) consists in the interaction of small-scale turbulent structures on the stagnation line of the bluff body. The result of this interaction is an

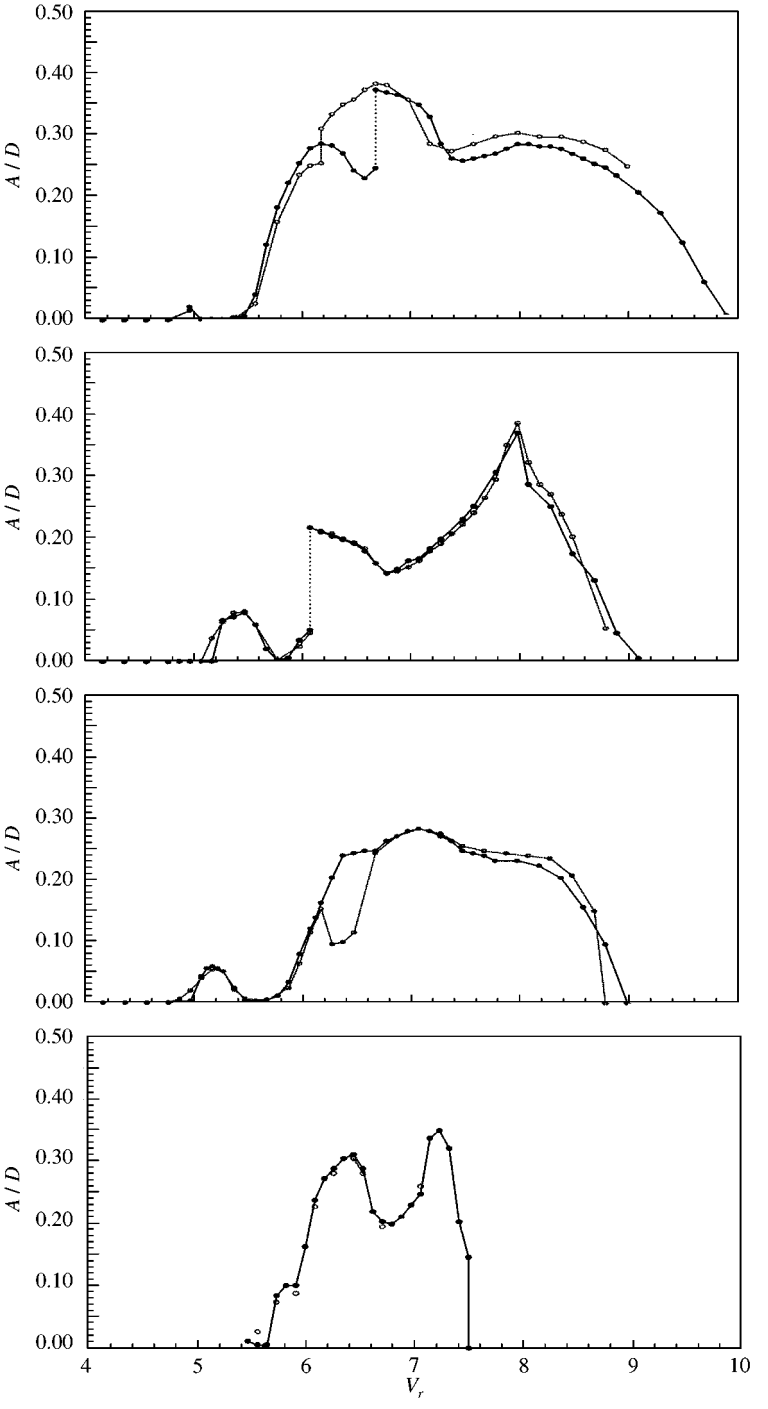

Figure 12. In-phase mechanical coupling ($\Theta_M = 0°$): the effect of the spacing ratio; from top, $L/D = 10$, 13, 16 and 25; ●: increasing velocity, ○: decreasing velocity.

increased mixing in the shear layer and its earlier re-attachment. As mentioned earlier, Nakamura has extended the mechanism to include the effect of large-scale turbulent structures on the organization of the wake vortices.

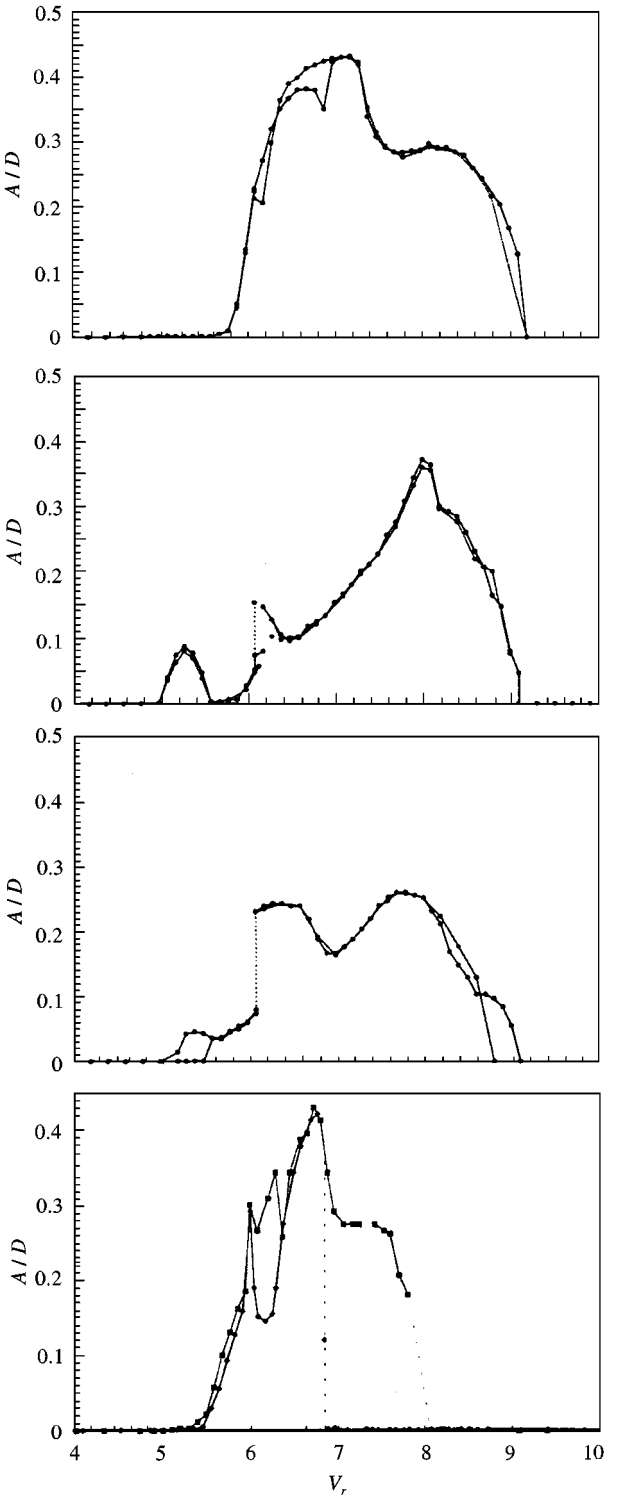

Figure 13. Out of phase mechanical coupling ($\Theta_M = 180°$): the effect of the spacing ratio; from top, $L/D = 10$, 13, 15 and 25; ○: decreasing velocity, ●: increasing velocity.

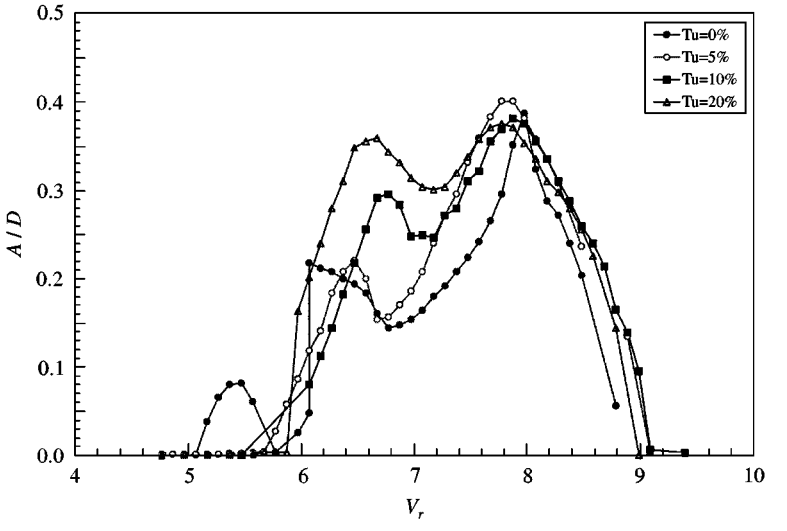

Figure 14. Effect of small-scale turbulence with different intensities ($L/D = 13$, $\Theta_M = 0°$).

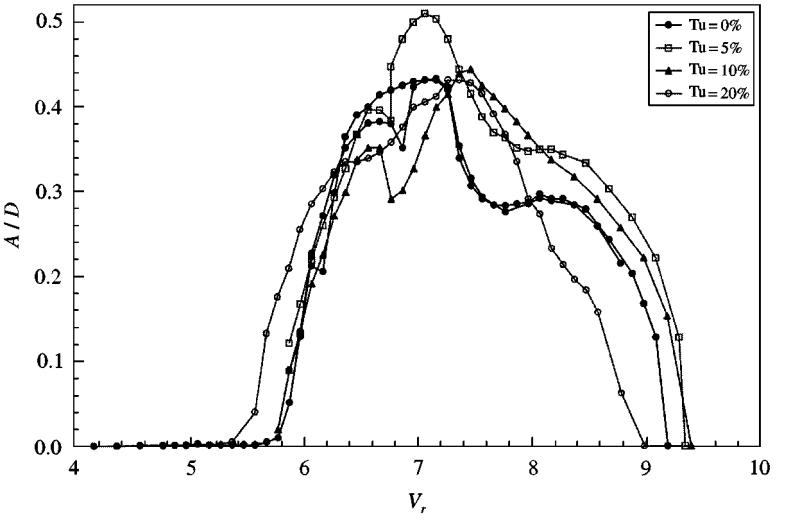

Figure 15. Effect of small-scale turbulence with different intensities ($L/D = 13$, $\Theta_M = 180°$).

The results of the present tests shown in Figures 14 and 15 for $L/D = 13$ agree with the following general observations. (i) Firstly, as the intensity of the external turbulence is increased, the formation of vortices in the near wake is sufficiently disturbed to eliminate the 2P mode of vortex shedding. This is inferred by the absence of the discontinuity in the tandem response at $V_r = 6{\cdot}17$ [Figure 14 ($\Theta_M = 0°$)] for turbulent intensities larger than the one in the empty wind tunnel. (ii) Secondly, the increase of the lift force with increasing value of the turbulence level, is deduced again in Figure 14 by the increase of the amplitude of vibration.

These two observations are valid for both the in-phase and out-of-phase vibrations of the tandem system. In the case of the out-of-phase vibrations, the phase angle Θ may be

a determining factor. Figure 15 shows a maximum amplitude $A/D = 0{\cdot}51$ occurring around $V_r = 7$ with Tu = 5%. This amplitude is even larger than the average between the maximum amplitude $A_1/D = 0{\cdot}38$ and $A_2/D = 0{\cdot}48$ around this velocity of the cylinders coupled only by fluid (see Figures 2 and 6). This agrees with the observations of Surry (1969) and Laneville and Parkinson (1971) showing the increase of the lift force with increasing value of the turbulence.

The present results differ, however, from those reported in Hardy & Van Dyke (1995) who observed an opposite effect in the case of transmission lines: the amplitude of vibration decreases with turbulence. This different behaviour is not explained but may be attributed to the effect of very low-frequency fluctuations of the velocity.

Curiously, with a turbulence intensity of 5%, the resonance velocity fluctuates between $V_r = 6{\cdot}65$ and $7{\cdot}35$, as shown in Figures 14 and 15. The lower limit ($V_r = 6{\cdot}65$) corresponds to the velocity for which $\Theta \approx 180^\circ$ and A_2/D has a maximum value 0·51.

The end of synchronization seems not to be greatly affected by turbulence when the coupled cylinders are vibrating in phase, but some effect can be observed in the case of out-of-phase vibration. For this last case, the end of synchronization reaches a maximum value at Tu = 5% and then decreases with increase of turbulence.

6. CONCLUSION

This experimental study shows that fluid and mechanical coupling as well as turbulence intensity greatly affect the dynamical response of a twin-cylinder bundle. This more complex response is explained in the light of preliminary investigations using the same experimental set-up. It generally exhibits a hysteresis, some discontinuities, and several velocities where the amplitude is maximum. The hysteresis and discontinuities are attributed to the presence of different modes of vortex shedding in the wakes of the cylinders.

When the cylinders are coupled only by fluid, the upstream cylinder behaves as an isolated one, while the downstream cylinder response depends on the separation between the cylinders. This response presents a hysteresis with two discontinuities concurring with those of the upstream cylinder, and a third discontinuity coinciding with the end of synchronization of the windward cylinder. The maximum amplitudes of oscillation and the synchronization region decrease with increasing value of the separation between the cylinders. The results showed also that the phase angle between the displacements of the cylinders is strongly dependent on the separation and the reduced velocity.

When the mechanical coupling is combined with the aerodynamic one, the response of the cylinders becomes even more complex. This response depends on the coupling mode and can be interpreted according to the results obtained when the cylinders are coupled only by fluid. The increase of turbulence is generally accompanied with an increase of the amplitude of vibration.

ACKNOWLEDGEMENTS

The authors would like to acknowledge the financial support of Hydro-Québec and the Natural Sciences and Engineering Research Council of Canada.

REFERENCES

BRIKA, D. & LANEVILLE, A. 1993 Vortex-induced vibrations of a long flexible circular cylinder, *Journal of Fluid Mechanics* **250,** 481–508.

BRIKA, D. & LANEVILLE, A. 1995 An experimental study of the Aeolian vibrations of a flexible circular cylinder vibrating at different incident planes. *Journal of Fluids and Structures* **9,** 371–391.

BRIKA, D. & LANEVILLE, A. 1996 A laboratory investigation of the aeolian power imparted to a conductor using a flexible circular cylinder. *IEEE Transactions on Power Delivery* **10,** 1045–1052.

BRIKA, D. & LANEVILLE, A. 1997 The power imparted by wind to a flexible circular cylinder in the wake of another stationary cylinder *IEEE Transactions on Power Delivery* **12,** 398–405.

BRIKA, D. & LANEVILLE, A. 1999 The flow interaction between a stationary cylinder and a downstream flexible cylinder. *Journal of Fluids and Structures* **13,** 579–606.

FENG, C. C. 1968 The measurement of vortex-induced effects in flow past stationary and oscillating circular and D-Section cylinders. M.A.Sc., thesis, University of British Columbia, Vancouver, Canada

HARDY, C. & VAN DYKE, P. 1995 Field observations on wind-induced conductor motions. *Journal of Fluids and Structures* **9,** 43–60.

LANEVILLE, A., GARTSHORE, I. S. & PARKINSON, G. V. 1975 An explanation of some effects of turbulence on bluff bodies, In *Proceedings 4*th *International Conference on Wind Effects on Buildings and Structures* (ed. K. J. Eaton), pp. 333–341. Cambridge University Press.

LANEVILLE, A. & PARKINSON, G. V. 1971 Effects of turbulence on galloping of bluff cylinders. In *Proceedings 3rd International Conference on Wind Effects on Buildings and Structures*, pp. 787–797. Tokyo.

NAKAMURA, Y. 1993, Bluff-body aerodynamics and turbulence. *Journal of Wind Engineering and Industrial Aerodynamics* **49,** 65–78.

NAKAMURA, Y. & OHYA, Y. 1986, Vortex shedding from square prisms in smooth and turbulent flows. *Journal of Fluid Mechanics* **164,** 77–89.

NAKAMURA, Y. & HIRATA, K. 1989, Critical geometry of oscillating bluff bodies *Journal of Fluid Mechanics* **208,** 375–393.

SURRY, D. 1969 The effect of high intensity turbulence on the aerodynamics of a rigid circular cylinder at subcritical Reynolds numbers UTIAS Report No 132, University of Toronto, Toronto, Canada.

WILLIAMSON, C. H. K. & ROSHKO, A. 1988 "Vortex formation in the wake of an oscillating cylinder", *Journal of Fluids and Structures* **2,** 355–381.

ZDRAVROVICH, M. M. 1982 Modification of vortex shedding in the synchronization range. *ASME Journal of Fluids Engineering* **104,** 513–517.